NJC

Accepted Manuscript

This is an *Accepted Manuscript*, which has been through the Royal Society of Chemistry peer review process and has been accepted for publication.

Accepted Manuscripts are published online shortly after acceptance, before technical editing, formatting and proof reading. Using this free service, authors can make their results available to the community, in citable form, before we publish the edited article. We will replace this *Accepted Manuscript* with the edited and formatted *Advance Article* as soon as it is available.

You can find more information about *Accepted Manuscripts* in the Information for Authors.

Please note that technical editing may introduce minor changes to the text and/or graphics, which may alter content. The journal's standard Terms & Conditions and the Ethical guidelines still apply. In no event shall the Royal Society of Chemistry be held responsible for any errors or omissions in this *Accepted Manuscript* or any consequences arising from the use of any information it contains.

ROYAL SOCIETY OF CHEMISTRY

www.rsc.org/njc

1

Receding mechanism of NLO Response of polyanion $[M_8O_{26}]^{4-}$(M=Cr, Mo, W) and the closed loops theory analysis

[a]Fujun Li, [a]Xiaojun Hu*, [b]Rongjian Sa and [c]Jing Feng

a, Key Lab. Of Regional Environment and Eco-Remediation, Ministry of Education, Shenyang University, Shenyang, Liaoning, 110044, China.

b, State Key Laboratory of Structural Chemistry, Fujian Institute of Research on the Structure of Matter, Chinese Academy of Sciences, Fuzhou, Fujian, 350002, China

c,College of Computer Science and Technology, Shenyang University of Chemical Technology, Shenyang, Liaoning, 110142, China.

ABSTRACT

The second hyperpolarizability of six octa-poly-oxo anions $[M_8O_{26}]^{4-}$(M=Cr, Mo, W) were studied by DFT/TDDFT method. All of the six high symmetric anions possess moderately large γ values and the results present a receding sign of the third order NLO response as the metal element changing from Mo to Cr and W. For the further knowledge of the third order NLO response mechanism, the electronic properties were studied by DFT method. The results suggest that the NLO property is closely related to the orbital closed loops of the unique electronic structure of polyanion cage, and the direct relationship of the third order NLO response with the number and shape of the loops is presented. It is the first try of the analysis of NLO response mechanism by "orbital closed loops theory".

Key words: polyoxometalate, the second hyperpolarizability, molecular orbital

* Corresponding author, Tel.: +86 2462268101; fax: +86 2462266533.
E-mail: hu-xj@mail.tsinghua.edu.cn

closed loops, density functional theory, NLO response

1. Introduction

Polyoxometalate cluster anions are the extended form of the polymerization of oxo-anions, and largely restricted to the Group 5 and 6 metals, vanadium, niobium, tantalum, molybdenum and tungsten. The range of cluster shapes, coordination modes, and metal ions lead to a large variety of possible structures and properties. Polyoxometalate cluster anions of Group 6, forming an extremely large and diverse group of compounds with remarkable chemical and physical properties[1,2], are used and have potential applications in catalysis, biology, medicine, optical, and magneto-chemistry, solid state technology, and chemical analysis [3～8]. Since the first clear evidence for the isomers of octamolybdate anion, $[Mo_8O_{26}]^{4-}$, was reported in 1970 in an infrared (IR) study by Schwing-Weill and Arnaud-Neu [9], there have been eight isomers reported successively, α-, β-, γ-, δ-, ε-, ζ-, η-, and θ-$[Mo_8O_{26}]^{4-}$[10-13]. The most important and common isomers are α- and β-octamolybdate. The conventional research studies of the two isomers have mainly been concentrating on Medicine, catalysis and new compound synthesis fields [14,15].

In recent years, some experimental studies of the polyoxomolybdate anions coordinated by organic ligands with moderately high Nonlinear Optical (NLO) response had been reported, focusing on the first hyperpolarizability [16,17], proving another high potential application of the polyoxoanions in nonlinear optical field. However, as always in high symmetric structures, “pure polyoxometalate structures”

without the coordination of ligands, almost never engender long-range charge transfers inner structure, and there rarely are research reports on the nonlinear optical properties of "pure-polyoxometalates".

Although the synthesis, structural and spectroscopic analysis, and the development of the applications of polyoxoanions are extremely rich areas of research, relatively few high-level computational studies have been reported, reflecting the intensive computational demands imposed by the large size of these species. Most of the first principle studies related to polyoxoanions have been proceeded by Poblet, Be ńard, and co-workers [18-20], at the Hartree-Fock (HF) level and the density functional theory (DFT) level, and by Bridgeman and Cavigliasso [21,22] and Borshch and coworkers[23,24] at the DFT level. A number of these studies related to the Keggin type anions [25,26]. Adam J. Bridgeman has completed a detailed study of the electronic structure of α- and β-$[Mo_8O_{26}]^{4-}$, with DFT method [27]. Great emphasis was placed on the detection of the molecular orbital "closed loops", which were formed by the metal centers and the bridging oxygen atoms linking the octahedral units. Nomiya and Miwa [28] have proposed that the number of such loops per MO_6 unit as a measure of the relative stability of the polyanion cages. We have recently completed a detailed study of the third order nonlinear optic properties and the electronic structures of α-, and β-isomers of octa-molybdate with DFT method at B3LYP level with ECP (effective core potential) triple-split basis set CEP-121g [29]. In that study, we found that the two high symmetric isomers own relatively large second hyperpolarizability, even though without coordination effect of any ligands.

We studied the electronic structures of the two isomers for the origination of the NLO response, and correlated the third order NLO response to the closed loops of the molecular orbital, and obtained a rational mechanism of the electronic changing effect on the NLO response.

In this paper, we succeeded the previous work. α- and β-isomers of polyoxoanions $[Cr_8O_{26}]^{4-}$ and $[W_8O_{26}]^{4-}$ were simulated theoretically based on the structures of α- and β-$[Mo_8O_{26}]^{4-}$, and the structures of $[Cr_8O_{26}]^{4-}$ and $[W_8O_{26}]^{4-}$ have not been realized by any experiments yet. The γ values were calculated by the finite field theory as an extension of the normal DFT runs of the energy calculations, and the geometric and electronic structures were studied for the origination of the NLO response. The molecular orbital "closed loops" theory was used for the analysis of the mechanism of the NLO response which receding as the metal core changing from Mo to Cr, and W, and a much clearer correlation between the closed loops and the NLO response was presented.

2. Computational methodology

The selection of the theoretical methods and computational models should meet the requirements of both accuracy and computing economy.

Density functional theory (DFT) has been widely used in most branches of chemistry, optical chemistry, biochemistry, and materials [30,31]. By DFT, all of the molecular properties are solely determined by the electron density, and is generally evaluated by solving the KohnSham equation which includes kinetic, Coulombic, exchange, and correlation terms. The choice of the XC functional is directly

correlated to the quality of the DFT results. Although the exact functional of DFT is still unknown, various alternative methods [32,33], together with various empirical corrections such as dispersion, have been successfully implemented in many popular computational codes.

B3LYP, a hybrid of exact Hartree-Fock exchange with local and semi-local exchange and correlation terms on the basis of the adiabatic connection [34-36], represents the most famous global hybrid GGA and has been used extensively in nearly all domains of chemistry. Without any optimization, B3LYP functional performs fairly well in the calculations of structures and energies of organic and inorganic compounds and chemical reactions. B3LYP as the most popular DFT method has dominated the DFT market for nearly 20 years. There are some literatures have reported that because of the incorrect long range charge transfer behaviors between the donor and acceptor, for the first hyperpolarizability calculation, the DFT-derived result sometimes overestimates the first hyperpolarizability of donor-π-conjugated bridge-acceptor (D-π-A) systems[37,38]. To overcome this problem, some long-rang-corrected functionals have been developed recently, Such as CAM-B3LYP [39], BHandHLYP[40] and LC-BLYP[41] etc. In this paper, the third order nonlinear optical property of the polyoxometalate ion structures were studied, and the mechanism of the NLO response was analyzed. Our calculations were based on the finite field theory, and the γ values were deduced on the energies of the structures in different extra electric field, in the expectation of avoiding the inherent fault of B3LYP. The quality of our results mostly depends on the accuracy of the

energy calculation, and B3LYP is a comparatively credible and efficient method to deal with the energy calculation of the relatively large structures of polyoxometalate ion systems [37].

Before the beginning of our work, a comparation of the second hyperpolarizability component γ_{mean} of the DFT-calculated results by several popular XC functionals is carried out. The XC functionals we selected were B3LYP, long-rang-corrected functional LC-BLYP and CAM-B3LYP, two modern DFT methods M06 (for main group thermochemistry, thermochemical kinetics, noncovalent interactions, excited states, and transition elements) and TPSS (charactered by non-empirical meta-generalized gradient approximation), respectively. Table1 shows the results of the γ_{mean} values. Comparing with the results of other XC functionals, the γ_{mean} by B3LYP is still overestimated a little, but is close to the average value, and that by the two modern DFT methods, TPSS and M06. Here, CAM-B3LYP and LC-BLYP do have the correcting effect on the overestimating error of B3LYP, but it is turned out that they may underestimate the γ_{mean} value too much.

Table1 comparation of γ_{mean} of $[Mo_8O_{26}]^{4-}$ without extra electric field

	B3LYP	CAM-B3LYP	LC-BLYP	TPSS	M06	average
$^a\gamma_{mean}(\times 10^{-35}$ esu)	7140	5938	5043	7090	6985	6448

$^a\gamma_{mean}=1/5[\gamma_{xxxx}+\gamma_{yyyy}+\gamma_{zzzz}+2(\gamma_{xxyy}+\gamma_{xxzz}+\gamma_{yyzz})]$

All the calculations of the six ion clusters were performed with the Amsterdam Density Functional (ADF2008) program [42]. As the six polyoxometalate clusters are relatively large molecules with octa-nuclear transition metal skeleton, the

relativistic effects and electron correlation were taken into account. The zero-order regular approximation (ZORA) [43] was adopted for each atom to account for the scalar relativistic effects.

All the geometric structures are optimized with the XC functionals based on the 1996 gradient-corrected correlation functional of Perdew, Burke and Ernzerhof (PBE) [44]. The frozen-core approximation was adopted on all the elements: The core orbitals of the non-metal elements O were frozen up to 1s, while those of Cr, Mo and W were frozen up to 2d, 3d and 4d, respectively. A standard valence triple-ζ STO basis set with valence polarization functions (TZVP) [45] was used. The second-order hyperpolarizabilities were calculated by the finite-field method. And the finite-field calculations were performed based on DFT energy runs at the hybrid functional B3LYP [35,36] level with ECP (effective core potential) triple-split basis set CEP-121g [46]. For the discussion of the origination of the NLO response, the vertical excitation energy were calculated by time dependent DFT (TDDFT) methods, and the UV-Vis absorption spectra were plotted with the Gaussian peak-shape modification by a width at half-height of 3000 cm^{-1}. In addition, the natural charge population and the bond valence were analyzed by NBO program [47].

3 Results and Discussion

3.1 Geometry structure

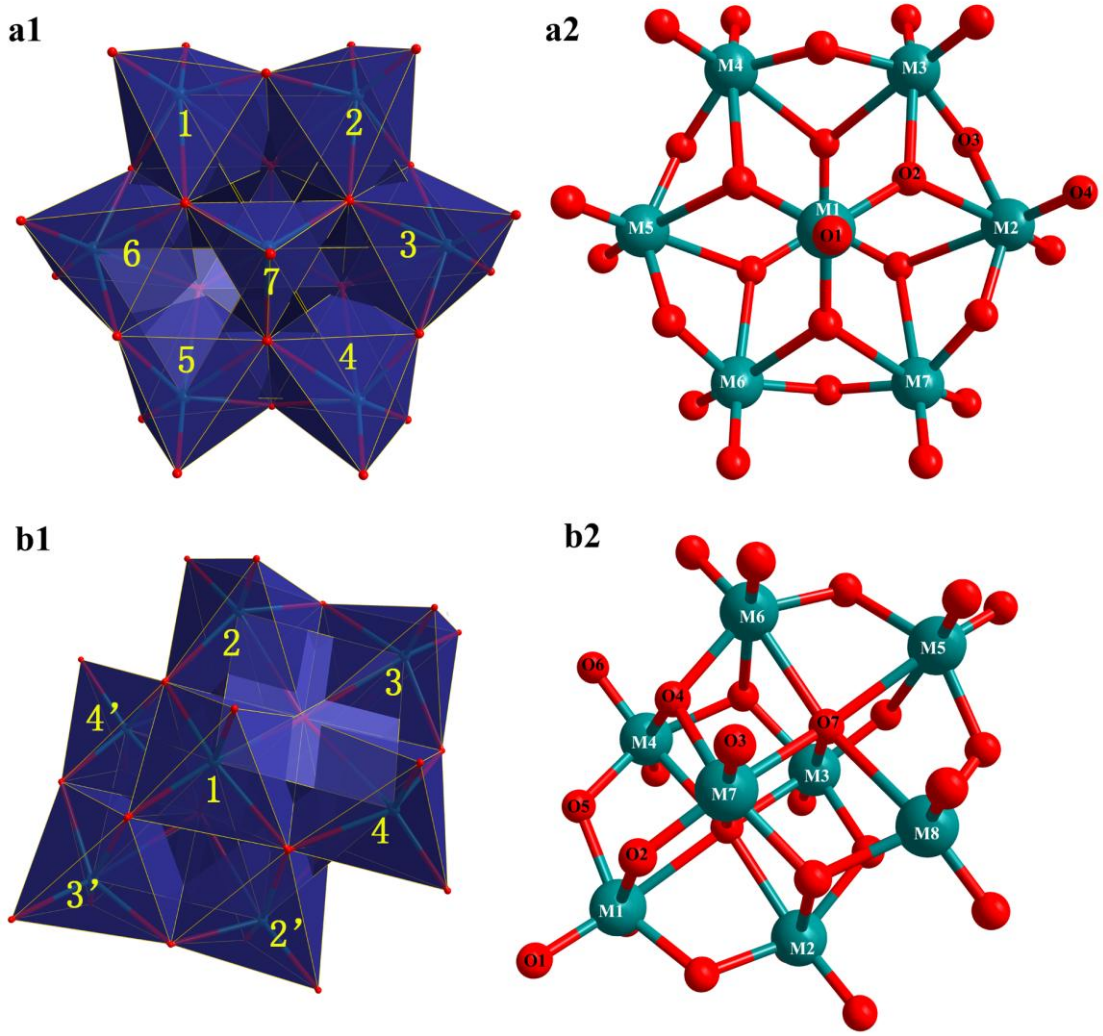

Fig.1. the structures of α- and β-$[M_8O_{26}]^{4-}$ (M=Cr, Mo, W) in polyhedron representation(a1,b1) and in ball and stick representation(a2,b2).

Figure1 shows the α- and β-$[M_8O_{26}]^{4-}$ ion structures in polyhedral representation (figure a1, b1), and ball-and-stick representation with the atom labeling schemes (figure a2, b2). The α-isomer, see figure a1, in approximate D_{3d} symmetry, consists of a ring of six MO_6 edge-shared octahedral bi-capped by MO_4 tetrahedral. The MO_6 and MO_4 units are distorted with short metal-oxygen terminal bonds as shown in figure a2, There are two types of metal atoms according to the coordination environment and

symmetric position, hexa-coordinated metal atoms in the six edge-shared octahedrons, labeled from M2 to M7 respectively, and tetra-coordinated metal atoms in the two tetrahedrons, labeled as M1 and M8 respectively. Meanwhile there are four types of oxygen atoms: two types of terminal bond oxygen O_t, include two O_t atoms in the tetrahedrons(O1), and twelve O_t atoms in the octahedrons(O4); two types of bridging oxygen, include six double bridging oxygen $O_{\mu 2}$ atoms (O3), and six triple bridging oxygen $O_{\mu 3}$ atoms(O2). The six $O_{\mu 2}$ atoms connect every two neighbor octahedrons and forming a six octahedral MO_6 units ring, and the six $O_{\mu 3}$ atoms shared by two of the six octahedral units and one tetrahedral MO_4 unit, connect the two MO_4 caps to the six octahedral units ring, and together with the $O_{\mu 2}$ atoms determine the shared edges of the neighbor octahedral units. Besides, there is a twelve- member ring, $[M_6O_6]$, composed of the six $O_{\mu 2}$ atoms and the six metal atoms of the MO_6 units presented. The β-$[M_8O_{26}]^{4-}$ structure, as shown in figure b1, consists of eight MO_6 groups of three distinct types, and these groups are edge-shared together forming the compact bilayer structure with approximate C_{2h} symmetry. The two layers of the structure are identical quadrangles parallel to each other, composed of four MO_6 groups. The corner superposition combines the two layers, and differentiates the MO_6 groups, forming three distinct types of the groups intra layer: the two groups, group1 and 3, along the corner superimposed direction and been across by σ_h symmetry plane form two types, and the other two groups, group2 and 4 form the third type. All the eight metal atoms are hexa-coordinated, and based on the symmetric position and coordination environment, see figure b2, there are three

types of metal atoms corresponding to the three types of the MO_6 groups respectively. The two metal atoms in the σ_h symmetry plane and belonging to group1 and 1' compose one type, labeled as M3 and M7; the other two metal atoms in the σ_h symmetry plane and belonging to group 3 and 3' compose the second type labeled as M1 and M5;the rest four metal atoms belonging to group2,2',4 and 4' compose the third type, labeled as M2,M4,M6 and M8 respectively. While the O atoms divide into 7 types, including fourteen O_t atoms of three types (O1, O3 and O6), four $O_{\mu 2}$ atoms (O5), two quasi-O_t atoms(O2), four $O_{\mu 3}$ atoms (O4), and two quintuple bridging oxygen $O_{\mu 5}$ atoms (O7). The bonds of the $O_{\mu 2}$ atoms together with two bonds of the $O_{\mu 3}$ atoms connecting the four groups intra layer and forming the quadrangle of the four MO_6 groups, and the bonds of the quasi-O_t atoms together with one bond of $O_{\mu 3}$ and $O_{\mu 5}$ atoms connecting the two layers. Besides, two parallel eight-member rings of two $O_{\mu 2}$ atoms, two $O_{\mu 3}$ atoms and four metal atoms, $[M_4O_4]$, are presented in the structure while the two $O_{\mu 5}$ atoms locate in the center of the two rings respectively, and shared by the four MO_6 groups

Table 2 lists the important values of the optimized parameters along with the experimental measured data of the polymolybdate anions. The optimized geometries are all in reasonable agreement with the experimental data. The molecular energies are also listed in table 2. The energies of the two isomers of $[Cr_8O_{26}]^{4-}$ and $[W_8O_{26}]^{4-}$ are low enough to confirm the stability and realizability of these simulated structures by DFT calculation.

Overall, compared to the α-structures, the β-isomers have to overcome steric

effects to exhibit such a tighter structure, and raised β-isomer higher molecular energy, as shown in table2. However, the energy difference between the two isomers is small. Considering the same charge population and approximate cluster size, the origination of the difference should be the coordination type and electronic structure, which we will discuss in the following sections in detail.

Table2 Selected optimized structure parameters compared with the crystallographically determined bond lengths and bond angles.

$[M_8O_{26}]^{4-}$ (M=Cr, Mo,W)			Bond length(Å)				Bond angle(°)	
		E_{tot}(au)	Mo-Ot_d	Mo-$O_{\mu 2}$	Mo-$O\mu_3$	Mo-$O_{\mu 5}$	∠$MoO_{\mu 3}$Mo	∠$MoO_{\mu 5}$Mo
α	Cr	-2648.57	1.618	1.814	2.481	-	83.3	-
	Mo	-2500.60	[a]1.735	[a] 1.933	[a] 2.505	-	[a] 87.3	-
			1.711	1.909	2.422	-	86.8	-
	W	-2499.23	1.759	1.941	2.513	-	87.8	-
β	Cr	-2648.58	1.762	1.943	1.995	2.394	109.0	85.7
	Mo	-2500.58	[b]1.746	[b]1.924	[b]1.951	[b]2.340	[b]111.5	[b]85.4
			1.695	1.976	1.966	2.374	112.0	86.3
	W	-2499.22	1.768	1.944	1.978	2.569	110.6	83.9

[a]the experimental data of α come from X-ray diffraction of ref. [48]. [b]the experimental data of β come from X-ray diffraction of ref. [49]

3.2 Electronic structure and the second hyperpolarizabilities

3.2.1 The second hyperpolarizabilities

The second hyperpolarizability of the six polyanions were calculated by finite field method as an extension of normal DFT run.

The molecule energy under a weak, homogeneous electric field can be expressed by the Buckingham type expansion [50]:

$$E(\vec{F}) = E(0,0,0) - \mu_i F_i - \tfrac{1}{2}\alpha_{ij}F_iF_j - \tfrac{1}{6}\beta_{ijk}F_iF_jF_k - \tfrac{1}{24}\gamma_{ijkl}F_iF_jF_kF_l - ..... \qquad (3.2.1.1)$$

And according to the symmetry, we simplify the formula to the following ones:

$$\gamma_{iiii}F_i^4 = -6E(0) - [E(2F_i) + E(-2F_i)] + 4[E(F_i) + E(-F_i)] \quad (3.2.1.2)$$

$$\gamma_{iijj}F_i^2F_j^2 = -4E(0) - [E(F_i, F_j) + E(-F_i, F_j) + E(F_i, -F_j) + E(F_i, -F_j)] + 2[E(F_i) + E(-F_i)] + 2[E(F_j) + E(F_j)] \quad (3.2.1.3)$$

$$\gamma_{mean} = 1/5[\gamma_{xxxx} + \gamma_{yyyy} + \gamma_{zzzz} + 2(\gamma_{xxyy} + \gamma_{xxzz} + \gamma_{yyzz})] \quad (3.2.1.4)$$

The formulas 3.2.1.2~3.2.1.4 were utilized to calculate the second hyperpolarizability of the six octa-polyoxometalate anions in this paper. Fields are added respectively along Cartesian axes. The choice of field strength is very important: The field must be large enough so that the contribution to the dipole moment expansion from the γ term is bigger than digital imprecision of the calculated dipole moment; at the same time, the field must be small enough so that the error incurred by the truncation of the expansion is acceptable [51,52]. Based on these considerations, for every field-added direction, the anions were respectively placed in 25 static external electric fields with different strength from 0.001au to 0.01au. Under the perturbation of the electric fields, 25 sets of the second hyperpolarizability tensors (γ_{iiii}, γ_{iijj}, and γ_{mean}) were deduced based on the results of the energy calculations of the anions. And the curves of the γ values changing with the field strength were plotted, and the most stable γ values on the convergence region were selected as the final results, as show in figure 2. According to the D_{3h} symmetry of the alpha isomers, the equations γ_{xxxx}= γ_{yyyy} =γ_{zzzz}, and γ_{xxyy}=γ_{xxzz}=γ_{yyzz} were obtained based on the formula 3.2.1.2 and 3.2.1.3, as shown in table3. Thus, only the converging curves of the third order nonlinear optical coefficients γ_{xxxx} and γ_{xxyy} were plotted to show that the second hyperpolarizability evaluated as the

fourth-order numerical derivatives of the energy are numerically stable with respect to the field amplitude. The symmetry of the beta isomers was similar to C_{2h}, and the converging curves of all the six γ components were plotted.

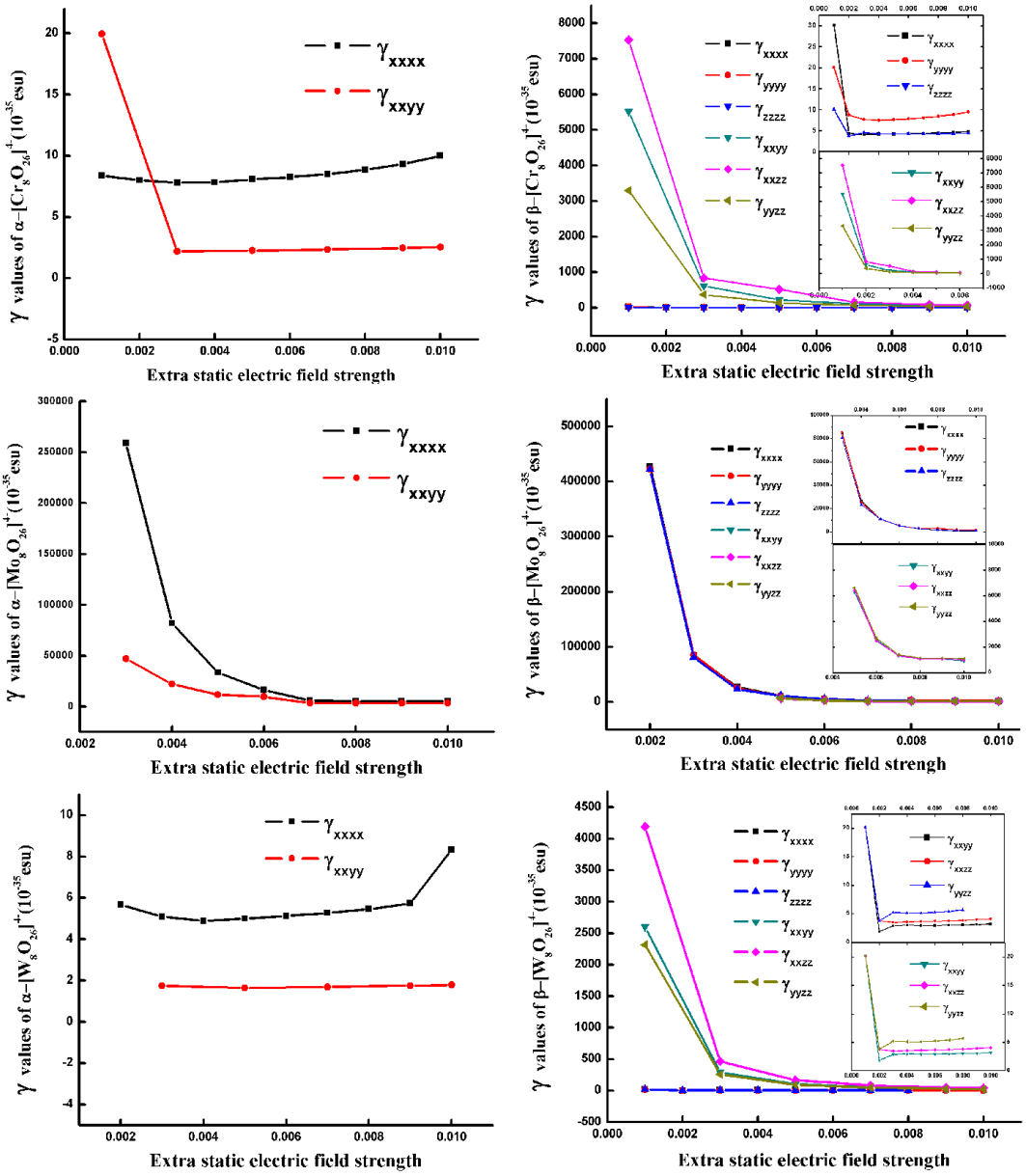

Fig.2. the converged curves of the second hyperpolarizability with respect to the field amplitude.

As can be seen from table3, all the six poly-anions exhibit the second static hyperpolarizability in moderate magnitude. The four simulated structures present much smaller γ values than the molybdate anions do, and the phenomenon is especially notable in α isomers. That means for both α and β isomers, the substitution of Mo atoms by W or Cr atoms makes the NLO response sign receding. As the three metal elements are in the same element group, possessing the similar electronic configuration, we conjecture that the number of the electron layers correlated with the number of *d* orbitals, plays the most important part in the origination of the third NLO response here.

Table3 The second static hyperpolarizability (unit: $\times 10^{-35}$ esu)

$[M_8O_{26}]^{4-}$		γ_{xxxx}	γ_{yyyy}	γ_{zzzz}	γ_{xxyy}	γ_{xxzz}	γ_{yyzz}	γ_{mean}
α	Cr	8.3	8.3	8.3	2.3	2.3	2.3	7.7
	Mo	5100.0	5100.0	5100.0	3400.0	3400.0	3400.0	7140
	W	5.0	5.0	5.0	1.8	1.8	1.8	5.2
β	Cr	4.9	9.5	4.4	613.0	837.0	366.0	730
	Mo	2849	2850.0	2853.0	1070.0	1060.0	1140.0	2586
	W	2.3	3.6	5.1	104.0	168.0	90.0	147
[a]$Cr(II)_4$		γ_{max}^{unit}=34000(a.u.)=1.7 $\times 10^{-35}$ esu						
[a]$Mo(II)_4$		γ_{max}^{unit}=129000(a.u.)=6.5 $\times 10^{-35}$ esu						
[b]C_{60}^-		240$\times 10^{-35}$ esu						
[c]C_{60}		3.7$\times 10^{-35}$ esu						

[a]γ values of one dimensional metal-metal bond compounds $Cr(II)_4$, $Mo(II)_4$ by UCCSD(T) method come from ref. [53]; [b]γ value of fullerene ion comes from ref [54]; [c]γ value of fullerene of neutral species comes from ref[55]

15

Transition-metal dinuclear complexes with metal–metal bonds have attracted great attention for decades because of their multiple $d\sigma$, $d\pi$, and $d\delta$ bonds resulting from the *d-d* orbital interactions. Nakano and his coworkers extended the concept of 'σ-dominant third-order NLO' obtained in dimetallic transition-meta systems to general one-dimensional polymetallic systems. Recently, Nakano and coworkers have published a few papers on one dimensional dimetal and tetrametal compounds, including $Cr(II)_2$, $Mo(II)_2$, Cr(II)4, $Mo(II)_4$ units[53]. The γ components of $Cr(II)_4$, $Mo(II)_4$ units are listed in table3, and they are much larger than those of the dimetals due to the $d\sigma$ electrons with an intermediate open-shell character of tetrametal compounds. What is interesting is that the γ components of Cr compounds are much smaller than that of Mo compounds, which also happened in our calculation results. Although there are no $d\sigma$, $d\pi$, and $d\delta$ bonds in the polyoxometalate ions structures, and the components of the valence bond are mainly σ, π and π^* bond from *d-p* orbital interactions, as shown in table 3, most of the γ components of the six polyoxometalate ions are larger than those of $Cr(II)_4$ and $Mo(II)_4$. The fullerene C_{60}, as a research hotpot of optics field, its third order NLO response is enhanced more than 65 times in its ion form C_{60}^-[54,55], and just about the γ value of β-$[Cr_8O_{26}]^{4-}$ and β-$[W_8O_{26}]^{4-}$, much smaller than those of α-, β-$[Mo_8O_{26}]^{4-}$ anions. The NLO response mechanism of the fullerene is attributed to its grant delocalized π bond and extra delocalized charge in its ion form. The polyoxometalate ion structures possess neither metal-metal bond nor delocalized large π bond, however they possess moderately large γ value, encouraging us to study the NLO response mechanism, and a promising NLO

response material is expected.

3.2.2 The absorption spectra analysis of the NLO response mechanism

Figure 3 shows the UV-Vis spectra of the six polyanions. The oscillator strength of the absorption peaks of the molybdate anions is much weaker than those of the other anions, and from Cr to W, the absorption peaks blue shift as the electron layers of the core metal increase, the peak of β-$[W_8O_{26}]^{4-}$ even shift out of the UV-Vis zone.

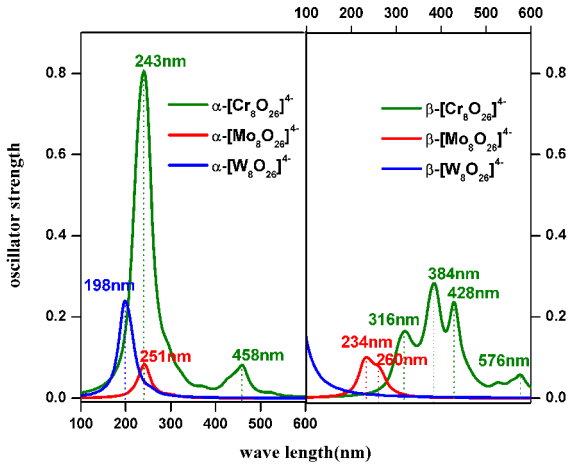

Fig.3 the UV-Vis spectra plotted with Gaussian peak-shape modification and by a width at half-height of 3000 cm^{-1}

Göller *et al.* based on an approximation of SOS theory [56], proposed the three-state model, correlating the second hyperpolarizability to three electronic states as follows:

$$\gamma_{iiii} = \frac{1}{6}\left[\frac{(r_{gm}^{i})^2(r_{mn}^{i})^2}{E_{gm}^2 E_{mn}} - \frac{(r_{gm}^{i})}{E_{gm}^3} + \frac{(r_{gm}^{i})^2 \Delta\mu_{gm}^2}{E_{gm}^3}\right] \qquad (3.2.2.1)$$

where $\Delta\mu_{gm}$ is the difference between the dipole moments of the states $|g>$ and $|m>$, E_{ik} are the transition energies, and r_{ij}^{k} are the Cartesian vector components of the transition dipole moments of the transition from state *i* to *j*.

According to the formula 3.2.2.1, we can get formula 3.2.2.2 following as,

$$\gamma_{iiii} = \frac{1}{6}\left\{\frac{(r_{gm}^{i})^2(r_{mn}^{i})^2}{E_{gm}^2 E_{mn}} + \frac{\Delta\mu_{gm}^2}{E_{gm}^3}\left[(r_{gm}^{i} - \frac{1}{2\Delta\mu_{gm}^2})^2 - \frac{1}{4\Delta\mu_{gm}^4}\right]\right\} \qquad (3.2.2.2)$$

For large γ tensors, it is obvious as shown by formula 3.2.2.2 that larger transition dipole moment and dipole moment change, and smaller energy gap are favored. Thus, absorption peaks appearing in the low energy zone with relatively high oscillation strength mean high NLO response. The transition dipole moments and energy change between the ground state and excited states corresponding to the absorption peaks of the UV-Vis spectrum of the six polyoxometalate ions are listed in table4 .

Table 4 the transition dipole moments and the energy difference between the ground state and the excited states and the major orbital transitions

$[M_8O_{26}]^{4-}$		$^{a}r^2_{mg}$	ΔE_{mg}(eV)	the major orbital transitions (weighting factor)			
α	Cr	0.4860	2.6930	126→141 (0.58)	59→144 (0.15)	61→137 (0.13)	70→170 (0.11)
		0.7862	5.1108	88→137 (0.27)	119→138 (0.11)	74→144 (0.11)	134→138 (0.11)
	Mo	0.2938	5.1283	129→140 (0.31)	136→151 (0.31)	76→142 (0.15)	95→150 (0.12)
	W	0.5604	6.3464	124→149 (0.26)	129→159 (0.20)	94→142 (0.10)	78→145 (0.10)
β	Cr	0.7629	2.1467	135→138 (0.24)	134→137 (0.21)	135→142 (0.15)	70→146 (0.11)
		1.6304	2.8878	136→138 (0.24)	134→137 (0.21)	135→138 (0.16)	78→137 (0.13)
		0.9052	3.2860	60→162 (0.10)	67→163 (0.11)	59→158 (0.10)	104→162 (0.10)

	Mo	0.1634 0.1560	4.7912 5.1730	126→143 (0.35) 86→153 (0.42)	124→163 (0.20) 61→137 (0.11)	135→143 (0.20) 59→143 (0.10)	65→137 (0.10) 60→143 (0.10)
	W	0.8222	9.2637	108→159 (0.21)	65→146 (0.11)	62→141 (0.10)	61→141 (0.10)

[a] $r^2_{mg}=r^2_x+r^2_x+r^2_x$

For the six ions, the two $[Cr_8O_{26}]^{4-}$ ions have the smallest energy gap, and the largest transition dipole moments, meanwhile, $[Mo_8O_{26}]^{4-}$ ions present the smallest transition dipole moments. However the γ tensors of $[Cr_8O_{26}]^{4-}$ are not the largest, but much smaller than those of $[Mo_8O_{26}]^{4-}$ ions. And the two $[W_8O_{26}]^{4-}$ ions possess the smallest γ tensors. From the results we can see that the mechanism of the third order NLO response of the polyoxometalate is very complicated, and the analysis based on SOS theory without the acquirement of the transition dipole moment and transition energy between two excited states in bi-photonic process is incomplete, however, the transition dipole moments and transition energies between excited states are hard to obtain by theoretical computation at present, reflecting the complication of the mechanism and the intense need of a more simple and systematic analyzing theory incorporated with full-scale impact factors. In this paper, the unique electronic structure of orbital closed loops by analysis provide some clues, and the analysis based on orbital closed loops theory is expected to give efficient insights for the NLO response mechanism in a new perspective.

3.2.3 Natural bond orbital analysis for the orbital closed loops discussion

The electron transfer processes of the structures were analyzed based on the natural bond orbital populations by NBO program, for the orbital closed loops discussion. Firstly, the natural charge population is exhibited here for the acquirement of the general tendency of the electron moving. The natural charge population of the anions is presented in figure 4. In the six structures, as discussed in section 3.1, the O atoms fall into four categories generally, according to the different coordination patterns, O_t, $O_{\mu 2}$, $O_{\mu 3}$, and $O_{\mu 5}$. For all of the six polyaninons, the negative charges distributed over the oxygen atoms, and the higher of the coordination number, the more of the negative charge concentrated. $O_{\mu 5}$ atoms concentrate the highest negative charge, proving the experience conclusion that the back bonding from *d* orbital of metals to anti-bonding orbital of ligands is the most important factor of the stabilization of metal complex molecules. Specially, O2 of β anions has been reported as quasi-terminal oxygen, whose character is between terminal oxygen O_t and bridging oxygen $O_{\mu 2}$, and in most cases was treaded as terminal oxygen [40]. The natural charge population of O2 in our study is also between that of O_t and $O_{\mu 2}$, more concentrated negative charge than terminal O atoms and less than $O_{\mu 2}$ atoms. As the metal core changing from Cr to W, both the negative charge and positive charge increasing, suggests the further separation of the opposite charges as the electron layer of metal atoms increase, and the more unstable of the anion structures.

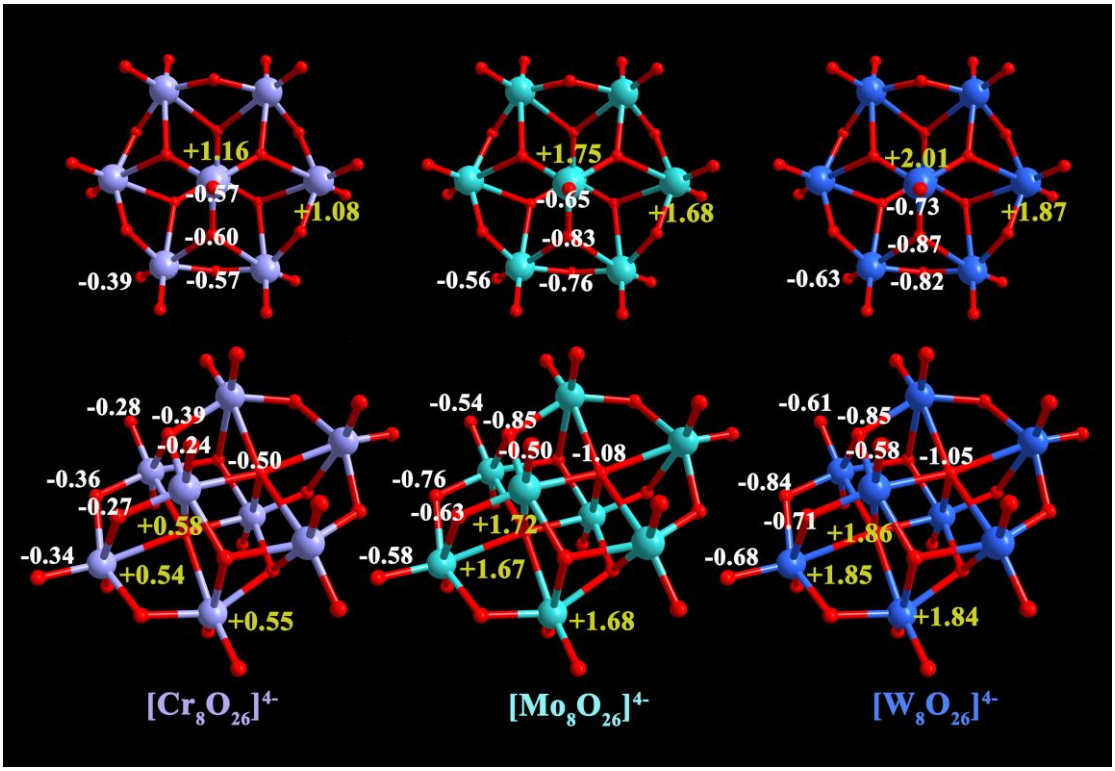

Fig.4. Natural charge population and electronic configuration

As can be seen from table5, the natural bond orbital analysis presents the bond compositions for all of the connection types. For the six isomers, all of these bonds are mainly composed of *d* orbital of metal atoms and *2p* orbital of O atoms, and the *2p* orbital of O atoms takes the most proportion. In addition, for the α isomers, *s*, *p* orbital of metal atoms also hold a little in the bonding, while for the β isomers, *s* orbital of Mo atoms and inner layer *1p* orbital of O atoms also hold a little in the bonding. What is noticeable is that the inner layer orbital of O atoms of the β isomers are activated in the bonding, and those of the α isomer are not; on the contrary, the inner layer orbital of Metal atoms of α isomers are activated deeper than those of β isomers. Referring to figure 4, the natural charge population suggests that the higher coordinate (μ^3 and μ^5) sites concentrate the higher charges and present significantly lower co-valences.

Table5 Natural bond orbital

	Bond type	α-$[Cr_8O_{26}]^{4-}$	α-$[Mo_8O_{26}]^{4-}$	α-$[W_8O_{26}]^{4-}$
O_t	M1-O1	$0.56(sp^{0.7}d^{9.4})_{Cr}+0.83(sp^{3.6})_O$ $0.49(p^1d^3)_{Cr}+0.87\ (p)_O$ ------	$0.49(sd^{2.7})_{Mo}+0.87(sp^{4.2})_O$ $0.38(pd^{2.5})_{Mo}+0.92\ (p)_O$ $0.38\ (pd^{2.5})_{Mo}+0.93(p)_O$	$0.51(sd^{2.7})_W+0.86(sp^{4.0})_O$ $0.42(pd^{6.5})_W+0.91\ (p)_O$ $0.43\ (pd^{7.9})_W+0.90(p)_O$
	M2-O4	$0.53\ (sp^{1.9}d^{16.0})_{Cr}+0.85(p)_O$ $0.54\ (sp^{0.3}d^{4.2})_{Cr}+0.84(sp^{3.2})_O$ ------	$0.39\ (sp^{2.0}d^{6.4})_{Mo}+0.92(sp^{7.6})_O$ $0.47\ (sp^{0.6}d^{4.1})_{Mo}+0.89(sp8.8)_O$ $0.46\ (pd^{3.4})_{Mo}+0.89(p)_O$	$0.46\ (spd^{2.7})_W+0.89(sp^{3.5})_O$ $0.39\ (pd^{3.4})_W+0.92(p)_O$ $0.46\ (pd^{3.6})_W+0.89(p)_O$
$O_{\mu 2}$	M2-O3	$0.49\ (sp^{0.6}d^{2.6})_{Cr}+0.87(sp^{4.8})_O$ $0.43\ (pd^{10.6})_{Cr}+0.90(p)_O$	$0.38\ (sp^{0.7}d^{2.9})_{Mo}+0.92(sp^{7.4})_O$ ------	$0.38\ (sp^{0.8}d^{3.2})_W+0.92(sp^{5.8})_O$ ------
$O_{\mu 3}$	M1-O2	$0.50(sp^{1.4}d^{4.8})_{Cr}+0.86(sp^{3.8})_O$ $0.49(pd^{7.6})_{Cr}+0.87(p)_O$ $0.49(pd^{8.1})_{Cr}+0.87(p)_O$	$0.40(sp^{0.9}d^{3.3})_{Mo}+0.92(sp^{4.9})_O$ $0.31(sp^{4.9}d^{13.6})_{Mo}+0.95(p)_O$ $0.33(pd^{3.6})_{Mo}+0.94(p)_O$	$0.42\ (sp^{0.2}d^{2.9})_W+0.91(sp^{5.4})_O$ $0.30\ (pd^{5.3})_W+0.95(p)_O$ ------
	M2-O2	$0.29\ (sp^{6.0}d^{6.3})_{Cr}+0.95(p)_O$	$0.19\ (sp^{0.2}d^{2.3})_{Mo}+0.98(p)_O$	$0.53\ (sp^{1.4}d^{2.5})_W+0.84(sp^{1.0})_O$
		β-$[Cr_8O_{26}]^{4-}$	β-$[Mo_8O_{26}]^{4-}$	β-$[W_8O_{26}]^{4-}$
O_t	M1-O1	$0.52(sd^{2.3})_{Cr}+0.85\ (sp^{6.4})_O$ $0.56\ (pd^{8.1})_{Cr}+0.83\ (p)_O$ -----	$0.46(sp^{0.3}d^{2.7})_{Mo}+0.89\ (sp^{3.4})_O$ $0.39\ (sp^{4.7}d^{15.2})_{Mo}+0.92(p)_O$ $0.47(pd^{2.6})_{Mo}+0.89\ (p)_O$	$0.51(sd^{3.4})_W+0.86\ (sp^{3.6})_O$ $0.39\ (pd^{2.3})_W+0.92\ (p)_O$ ------
	M4-O6	$0.51(sp^{0.2}d^{2.2})_{Cr}+0.86\ (sp^{3.9})_O$ $0.58\ (pd^{9.9})_{Cr}+0.81\ (p)_O$ ------	$0.50(sd^{2.3})_{Mo}+0.87\ (sp^{2.9})_O$ $0.47(pd^{1.7})_{Mo}+0.88\ (p)_O$ ------	$0.50(sd^{2.6})_W+0.87\ (sp^{3.2})_O$ $0.49(d)_W+0.87\ (p)_O$ $0.47(pd^{3.3})_W+0.88\ (p)_O$
	M7-O3	$0.48(sp^{2.4}d^{4.0})_{Cr}+0.88(sp^{4.8})_O$ $0.58(pd^{7.2})_{Cr}+0.82(p)_O$ $0.53(sp^{2.1}d^{12.3})_{Cr}+0.85(sp^{14.8})_O$	$0.49(sd^{2.5})_{Mo}+0.87(sp^{3.1})_O$ $0.47(pd^{2.5})_{Mo}+0.88\ (p)_O$ $0.52(d)_{Mo}+0.85\ (p)_O$	$0.51(sd^{2.9})_W+0.86(sp^{3.0})_O$ $0.46(pd^{3.2})_W+0.89\ (p)_O$ $0.40(pd^{3.4})_W+0.92\ (p)_O$
$O_{\mu 2}$	M7-O2	$0.44(sp^{1.9}d^{1.9})_{Cr}+0.90(sp)_O$ $0.59(pd^{16.3})_{Cr}+0.81(p)_O$	$0.46(sd^{2.0})_{Mo}+0.89\ (sp^{2.7})_O$ $0.49(pd^{5.0})_{Mo}+0.87\ (p)_O$	$0.40(sd^{3.0})_W+0.92\ (sp^{3.0})_O$ $0.46(pd^{5.6})_W+0.89(p)_O$
	M1-O2	$0.28(sp^{5.3}d^{2.0})_{Cr}+0.96(sp)_O$	Weak bond	$0.22(sp^{2.3}d^{2.3})_W+0.98\ (p)_O$
	M1-O	$0.44(sp^{2.0}d^{2.3})_{Cr}+0.90\ (sp^{1.5})_O$	$0.39(spd^{3.1})_{Mo}+0.92\ (sp7.^4)_O$	$0.39(sp^{0.6}d^{2.9})_W+0.92\ (sp^{5.8})_O$
$O_{\mu 3}$	M7-O4	$0.45(sp^{2.0}d^{2.6})_{Cr}+0.89\ (sp^{5.3})_O$	$0.37(sp^{1.2}d^{3.2})_{Mo}+0.93\ (sp^{5.3})_O$	$0.37(spd^{3.1})_W+0.93\ (sp^{5.5})_O$
$O_{\mu 5}$	M3-O7	$0.31(sp^{9.1}d^{4.2})_{Cr}+0.91\ (sp^{2.3})_O$	Weak bond	Weak bond
	M7-O7	$0.43(sp^{3.3}d^{2.7})_{Cr}+0.91\ (sp^{1.5})_O$	Weak bond	$0.33(spd^{3.6})_W+0.94\ (sp^{4.6})_O$

3.2.4 The molecular orbital "closed loops" theory on the second hyperpolarizability

By the NBO analysis, the main charge transfer processes with the energy change of the structures accompanied are exhibited in this study. The orbital interactions

separate the electronic structures of the anions into several electron delocalized units. The electronic structure of α-$[Cr_8O_{26}]^{4-}$ are separated into five units: the two $[CrO_4]$ caps compose two units ($^{Cr}U1_\alpha$, $^{Cr}U2_\alpha$), and every two neighborhood $[CrO_6]$ groups in the ring compose one unit, forming three units ($^{Cr}U3_\alpha$, $^{Cr}U4_\alpha$, $^{Cr}U5_\alpha$) in total. The charge transfer with the maximum energy lowing (1000J) are the interactions of the anti bond Cr-$O_{\mu 2}$ with the anti bond Cr-O_t and lone pair orbital of Cr atoms, inner $^{Cr}U3_\alpha$, $^{Cr}U4_\alpha$ and $^{Cr}U5_\alpha$ units. The maximum transfer energy between the different units is about 60J. The electronic structure of α-$[Mo_8O_{26}]^{4-}$ divide into two units: one of the $[MoO_4]$ caps, form a unit, $^{Mo}U1_\alpha$, and the other unit is composed of the ring of the six $[MoO_6]$ units and the other $[MoO_4]$ cap, $^{Mo}U2_\alpha$. The maximum charge transfer energy is 900J, and the transfer is from the anti bond Mo-$O_{\mu 3}$ to the anti bond Mo-O_t inner $^{Mo}U2_\alpha$. The maximum transfer energy between the two units is about 20J. As for α-$[W_8O_{26}]^{4-}$, there are three units presented in the electronic structure: the two $[WO_4]$ caps form two units ($^{W}U1_\alpha$, $^{W}U2_\alpha$), and the ring of the six $[WO_6]$ groups forms the third units ($^{W}U3_\alpha$). The maximum charge transfer energy is only 300J, and the maximum transfer energy between different units is only about 10J. For β-$[Cr_8O_{26}]^{4-}$ and β-$[W_8O_{26}]^{4-}$ anion, the whole electronic structure is kept in one unit, and not separated. The maximum charge transfer energy is much larger, about 3000J and 5000J respectively. While for β-$[Mo_8O_{26}]^{4-}$, the electronic structure is separated into four electronic units: the two parallel rings of the four $[MoO_6]$ groups compose two units ($^{Mo}U1_\beta$, $^{Mo}U2_\beta$), and the two $O_{\mu 5}$ atoms at the center of each ring compose the other two units ($^{Mo}U3_\beta$, $^{Mo}U4_\beta$) independently. The maximum charge transfer energy

is about 900J, and the maximum transfer energy between two units is about 50J.

Table 6 Charge transfer energy and orbital closed loops count

	α-$[M_8O_{26}]^{4-}$			**β**-$[M_8O_{26}]^{4-}$		
	Cr	Mo	W	Cr	Mo	W
$^{a}E_{max}$(J)	1000	900	300	3000	900	5000
Electron unit count	5	2	3	1	4	1
Loops count	5	6	4	5	5	5
$^{b}E_{l\text{-}u(l\text{-}l)}$(J)	60	20	10	------	50	------
γ_{mean}(10^{-35}esu)	7.7	7140	5.2	730	2586	147

^{a}the maximum charge transfer energy; ^{b}the maximum energy of charge transfer between the orbital loops of different electronic units, or the loops and the electronic units.

The maximum charge transfer energy, the maximum energy of charge transfer between the electronic units, orbital closed loops of different units, or between the loops and electronic units for all the six anions are listed in table6, with the number of the orbital closed loops, electronic units, and the corresponding γ_{mean} value. It is obvious that the structures with charge transfer of more molecular orbital closed loops present larger hyperpolarizability. In addition, the existing pattern, range and shape of the orbital closed loops are the other important factors affecting the NLO response. Figure5 and 6 show the molecular orbital graphs possessing orbital closed loops, with orbital numbers. Table4 lists the main transition orbital pairs, corresponding to the absorption peaks. Since the complexity of the electronic structure of the compound containing transition metals, not all the orbital pairs contributing to the absorption peaks are listed. Most of the orbital shown in figure5 and 6 can be found in table 4, which means that these orbital may not contribute the

most, but can play important effect in the NLO response origination.

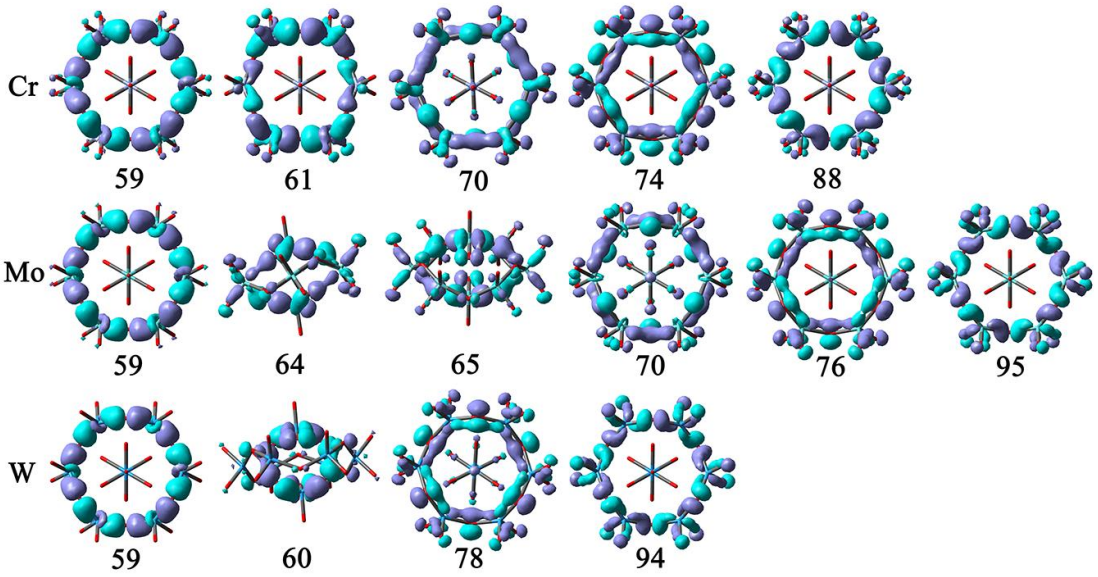

Fig.5. the molecular orbital closed loops of α-$[M_8O_{26}]^{4-}$(M=Cr, Mo,W)

For the alpha isomers, the molybdate anion possesses the most molecular orbital closed loops, see figure5. Four loops are along the twelve-member ring $[Mo_6O_6]$, all in the electronic unit $^{Mo}U2_{\alpha}$. The other two loops vertically cross the ring, made up of the atoms in the two $[MoO_4]$ caps and two $[MoO_6]$ groups of the ring, and involve in both of the two electronic units $^{Mo}U1_{\alpha}$ and $^{Mo}U2_{\alpha}$. The five loops of the chromate anion are all along the twelve-member ring $[Cr_6O_6]$, and involve in the three electronic unites $^{Cr}U3_{\alpha}$, $^{Cr}U4_{\alpha}$ and $^{Cr}U5_{\alpha}$. The tungstate anion possesses four loops, and three of the loops form along the $[W_6O_6]$ ring in the electronic unit $^{W}U2_{\alpha}$, the other one are formed by the atoms in the two $[WO_4]$ caps of $^{W}U1_{\alpha}$ and $^{W}U3_{\alpha}$ electronic units separately.

25

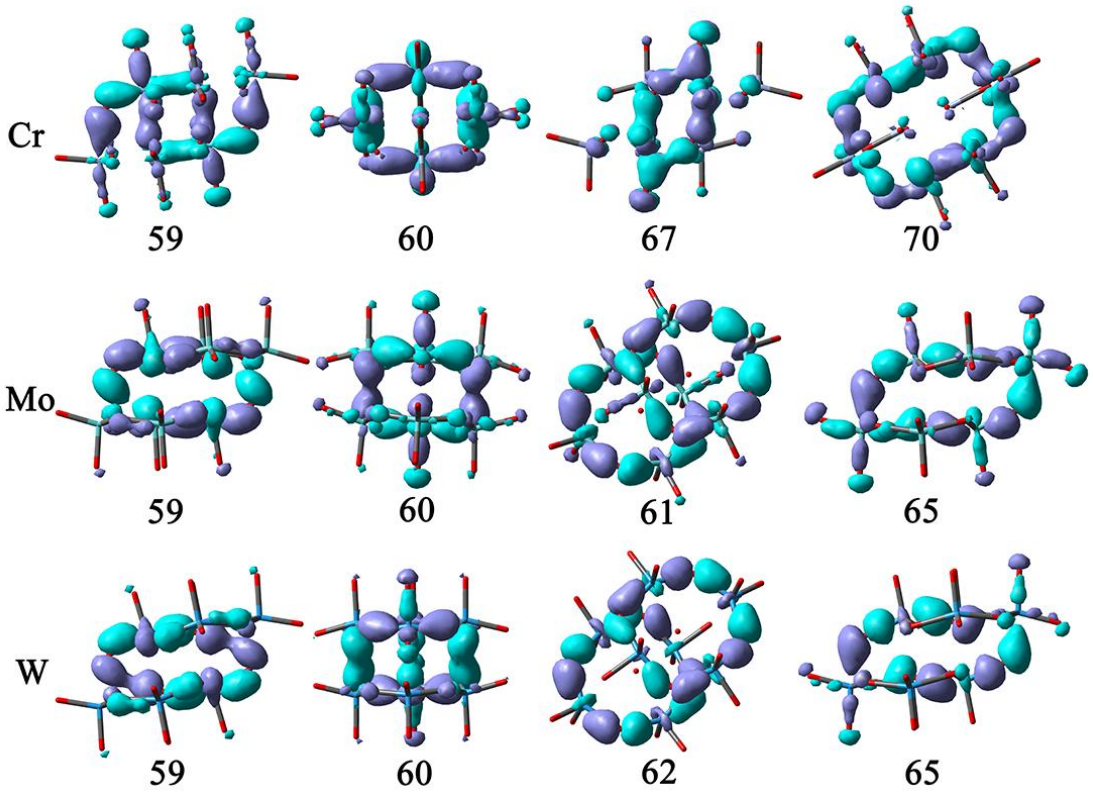

Fig.6. the molecular orbital closed loops of β-$[M_8O_{26}]^{4-}$(M=Cr, Mo,W)

Figure 6 shows the molecular orbital closed loops of the β isomers. For every of the three β isomers, four orbital present the character of closed loops, and one of the four orbital possesses two parallel closed loops, meaning that all the β isomers possess five loops. The whole electronic structure of the chromate anion and tungtate anion are kept in one electronic unit. The 67th orbital of the chromate anion contains two closed loops of six atoms, which across the two parallel $[Cr_4O_4]$ rings and parallel to each other. As for the tungstate anion, two closed loops form along the two parallel $[W_4O_4]$ rings in the 62nd orbital and parallel to each other. The electronic structure of the molybdate anion divides into four electronic units, and the 61st orbital has two closed loops forming along the two parallel $[Mo_4O_4]$ rings which

belong to the two electronic units $^{Mo}U1_{\beta}$ and $^{Mo}U2_{\beta}$ separately. In overall, molecular orbital closed loops of the three β isomers are similar in number and shape: every of the β isomers has five loops, and two of the loops are in the same molecular orbital, meanwhile, the other three loops are all across the two parallel $[M_4O_4]$ rings with similar shape except 70th orbital of chromate anion. The differences are presented in that the range of the 59th orbital loop of the molybdate anion is little larger than those of the chromate and tungtate anions, and the two parallel loops of molybdate anion in one molecular orbital are belongs to two different electronic units separately, keeping entire.

In conclusion, firstly, the number sequence of the molecular orbital closed loops can be presented as α-$[Mo_8O_{26}]^{4-}$(6)> α-$[Cr_8O_{26}]^{4-}$(5), β-$[Cr_8O_{26}]^{4-}$(5), β-$[Mo_8O_{26}]^{4-}$(5), β-$[W_8O_{26}]^{4-}$(5)> α-$[W_8O_{26}]^{4-}$(4); secondly, the sequence of the largest closed loops number in one orbital is β-$[Cr_8O_{26}]^{4-}$(2), β-$[Mo_8O_{26}]^{4-}$(2), β-$[W_8O_{26}]^{4-}$(2)> α-$[Cr_8O_{26}]^{4-}$(1) α-$[Mo_8O_{26}]^{4-}$(1), α-$[W_8O_{26}]^{4-}$ (1), finally, the sequence of the number of the electronic units with intact closed loops is β-$[Mo_8O_{26}]^{4-}$(2)> α-$[Mo_8O_{26}]^{4-}$(1), α-$[W_8O_{26}]^{4-}$(1), β-$[Cr_8O_{26}]^{4-}$(1), β-$[W_8O_{26}]^{4-}$(1)> α-$[Cr_8O_{26}]^{4-}$(0). Based on the three molecular orbital closed loops sequence, the second hyperpolarizability of the six polyanion are analyzed. According to the first sequence, the anion α-$[Mo_8O_{26}]^{4-}$ has the largest closed loops number and α-$[W_8O_{26}]^{4-}$ has the smallest, meanwhile, α-$[Mo_8O_{26}]^{4-}$ possesses the largest γ_{mean} value, and α-$[W_8O_{26}]^{4-}$ posseses the smallest; then according to the second sequence, the largest closed loops numbers in one orbital of the three β isomers are larger than

that of α-$[Cr_8O_{26}]^{4-}$, meanwhile the γ_{mean} values of the three β isomers are larger than that of α-$[Cr_8O_{26}]^{4-}$; based on the last sequence, the number of the electronic units with intact closed loops of β-$[Mo_8O_{26}]^{4-}$ are larger than those of β-$[Cr_8O_{26}]^{4-}$ and β-$[W_8O_{26}]^{4-}$, meanwhile γ_{mean} value of β-$[Mo_8O_{26}]^{4-}$ are larger than those of β-$[Cr_8O_{26}]^{4-}$ and β-$[W_8O_{26}]^{4-}$. Thus, the sequence of the third order NLO coefficients is obtained based on the three closed loops sequence as α-$[Mo_8O_{26}]^{4-}$ > β-$[Mo_8O_{26}]^{4-}$ > β-$[Cr_8O_{26}]^{4-}$, β-$[W_8O_{26}]^{4-}$ > α-$[Cr_8O_{26}]^{4-}$> α-$[W_8O_{26}]^{4-}$, in good agreement with the sequence of γ values by the finite field calculation of the second hyperpolarizability.

Thus, the molecular orbital "closed loops" theory is a novel and efficient analysis method of the origination of the third order NLO response, special to these cage structure of polyoxometalate anions.

4 conclustion

In this work, we applied high-level DFT methods to study the third order nonlinear optical response of the six octa-polyoxometalate anions of group VI metals, Cr, Mo, and W. The geometric structures of α- and β-isomers of $[Cr_8O_{26}]^{4-}$ and $[W_8O_{26}]^{4-}$ were theoretical simulated based on the two isomers of $[Mo_8O_{26}]^{4-}$. The results of the study on the thermo stability suggest that the four simulated structures are stable and realizable, and from Cr to W, as the electron layers increase, the polyoxometalate anions become unstable. The second hyperpolarizability were calculated by finite field method as an extension of an usual DFT energy run. The

results suggest that all of the polyanions exhibit relatively large NLO response. Furthermore, the molecular orbital "closed loops" theory for the molecular stabilization analysis by Particular, Nomiya and Miwa is used in our work to understand the mechanism of the different NLO response behaviors of the anions. We present a thorough and efficient analysis method for the origination of the third order NLO response in electronic structure aspect, and we hope this method will provide helpful reference for the researchers of theoretical chemistry field and nonlinear optics field.

Acknowledgements

This work has been supported by National Natural Science Foundation of China (21277093), Program for New Century Excellent Talents in University (NCET-13-0910) and the Science and Technology Program of Shenyang City of China (F13-062-2-00). We also acknowledge the computer facility in the Virtual Laboratory for Computational Chemistry and Supercomputing Center of CNIC in Beijing.

References

[1] M.T. Pope, Heteropoly and Isopoly Oxometalates, Springer-Verlag: Heidelberg, 1983.

[2] M.T. Pope, A. Muller, Angew. Chem., Int. Ed. Engl. 30(1991)34-48.

[3] L.C.W. Baker, D.C. Glick, Chem. ReV. 98(1998)3-50.

[4] M.T. Pope, A. Mu ̈ller, Polyoxometalates: from Platonic Solids to Anti-Retroviral

Activity, Kluwer: Dordrecht, 1994.

[5] J.T. Rhule, C.L. Hill, D.A. Judd, Chem. Rev., 98(1998)327-358.

[6] U. Kortz, F. Hussain, M. Reicke, Angew. Chem. Int. Ed., 44(2005)3773-3777.

[7] S.S. Mal, U. Kortz, Angew. Chem. Int. Ed., 44 (2005)3777-3780.

[8] Y. Yang, M.H. Cao, C.W. Hu, Y.H. Guo, E.B., J. Nanosci. Nanotechnol., 4(2004)833-837.

[9] M. J. Schwing-Weill, F. Arnaud-Neu, Bull. Soc. Chim. Fr.,(1970)853-860.

[10] V.G. Gregoriou, S.E. Rodman, B.R. Nair, P.T. Hammond, J. Phys. Chem. B, 106 (2002)11108-11113.

[11] S. Sasic, D.A. Clark, J.C. Mitchell, M.J. Snowden, Appl. Spectrosc., 59(2005) 630-638.

[12] M.L. Niven, J.J. Cruywagen, and J.B.B. Heyns, J. Chem. Soc., Dalton Trans., 19 (1991)2007-2011.

[13] J.Q. Xu, R.Z. Wang, G.Y. Yang, Y.H. Xing, D.M. Li, W.M.Bu, L. Ye, Y.G. Fan, G.D. Yang, Y. Xing, Y.H. Lin and H.Q. Jia, Chem. Commun., 35(1999)983-984.

[14] C.D. Wu, C.Z. Lu, X. Lin, H.H. Zhuang, J.S. Huang, Inorg. Chem. Commun., 5 (2002)664-665.

[15] H.Y. Zang, D.Y. Du, S.L. Li, Y.Q. Lan, G.S. Yang, L.K. Yan, K.Z. Shao, Z.M. Su, J. Solid State Chem., 184(2011)1141-1147.

[16] L.H. Zhang, Y. Wang, F. Ma, C.G. Liu, J. Organomet. Chem., 716 (2012)245-251.

[17] M.R.S.A. Janjua, M.U. Khan, B. Bashir, M. A. Iqbal, Y.Z. Song, S.A.R. Naqvi, Z.

A. Khan, Comput. Theor. Chem., 994(2012)34-40.

[18] M.M. Rohmer, R. Ernenwein, M. Ulmschneider, R. Wiest, M. Be ńard, Int. J. Quantum Chem., 40 (1991) 723-743.

[19] J.Y. Kempf, M.-M. Rohmer, J.M. Poblet, C. Bo, M. Be ńard, J. Am. Chem. Soc., 114(1992)1136-1146.

[20] J. M. Maestre, X. Lopez, C. Bo, J.M. Poblet, Inorg. Chem., 41(2002)1883-1888.

[21] A. J. Bridgeman, G. Cavigliasso, Polyhedron, 20(2001)2269-2277.

[22] A. J. Bridgeman, G. Cavigliasso, Chem. Phys., 279 (2002)143-159.

[23] H. Duclusaud, S. A. Borshch, J. Am. Chem. Soc., 123 (2001)2835-2838.

[24] S. A. Borshch, H. Duclusaud, J. M. M. Millet, Appl. Catal. A, 200(2000)103-108.

[25] J. M. Maestre, X. Lo´pez, C. Bo, J. M. Poblet, N. Casan˜-Pastor, J. Am. Chem. Soc., 123(2001)3749-3758.

[26] M.M. Rohmer, M. Be ńard, J.P. Blaudeau, J. M. Maestre, J. M. Poblet, Coord. Chem. ReV., 178 (1998)1019-1049.

[27] A. J. Bridgeman, G. Cavigliasso, Inorg. Chem., 41 (2002)3500-3507.

[28] K. Nomiya, M. Miwa, Polyhedron, 3(1984)341-346.

[29] F.J. Li, X.J. Hu, R.J. Sa, Mol. Phys., 111(2013)3081-3086.

[30] W. Kohn, A.D. Becke, R.G. Parr, J. Phys. Chem., 100 (1996)12974–12980.

[31] K. Burke, J. Chem. Phys., 136 (2012)150901.

[32] S.F. Sousa, P.A. Fernandes, M.J. Ramos, J. Phys. Chem. A, 111(2007)10439–10452.

[33] M. Korth, S. Grimme, J. Chem. Theory Comput., 5 (2009)993–1003.

[34] J. Harris, Phys. Rev. A, 29(1984)1648–1659.

[35] P.J. Stephens, F.J. Devlin, C.F. Chabalowski, M.J. Frisch, J. Phys. Chem., 98(1994)11623-11627.

[36] A.D. Becke, J. Chem. Phys., 98(1993)5648-5652.

[37] L.H. Zhang, Y. Wang, F. Ma, C.G. Liu, J. Organomet. Chem., 716(2012) 245-251.

[38] L.L. Lu, H. Hua, H. Hou, B.S. Wang, Comput. Theor. Chem., 1015 (2013) 64–71.

[39] T. Yanai, D. Tew, and N. Handy, Chem. Phys. Lett., 393(2004)51-57.

[40] A. D. Becke, J. Chem. Phys., 98 (1993)1372-1377.

[41] H. Iikura, T. Tsuneda, T. Yanai, and K. Hirao, J. Chem. Phys., 115 (2001)3540-44.

[42] C. F. Guerra, O. Visser, J.G. Snijders, G. te Velde, E.J. Baerends, in: E. Clementi, C. Corongiu (Eds.), STEF, Calgary, 1995, p. 303.

[43] E.V. Lenthe, E. J. Baerends, J.G. Snijders, J. Chem. Phys., 99(1993)4597-4610.

[44] J. P. Perdew, K. Burke, M. Ernzerhof, Phys. Rev. Lett., 77(1996)3865-3868.

[45] Schaefer, C. Huber, R. Ahlrichs, J. Chem. Phys., 100(1994)5829-5835.

[46] T.R. Cundari, W. J. Stevens, J. Chem. Phys., 98(1993)5555-5565.

[47] E. D. Glendening, J, K. Badenhoop, A. E. Reed, J. E. Carpenter, J. A. Bohmann, C. M. Morales, and F. Weinhold, ***NBO5.0*** Theoretical Chemistry Institute, University of Wisconsin, Madison (2001)

[48] T.C. hsieh, S.N.Shaikh, J.Zubieta, Inorg. Chem., 26(1987)4079-4089.

[49] X.J. Wang, B.S. Kang, C.Y. Su, K.B. Yu, H.X. Zhang, Z.N. Chen, Polyhedron, 18(1999)3371-3375.

[50] K. H., Tytko, J., Mehmke, S., Fischer, Struct. Bonding, (Berlin) 93(1999)129.

[51] A.D. Buckingham, J. Chem. Phys., 30 (1959)1580-1585.

[52] P. Calaminici, K. Jug, and A. M. Köster, J. Chem. Phys., 109(1998)7756-7763.

[53] H. Fukui, M. Nakano, B. Champagne, Chem. Phys. Lett., 527(2012)11-15.

[54] R. Lascola, J.C. Wright, Chem. Phys. Lett., 269(1997)79-84.

[55] L. Geng, J.C. Wright, Chem. Phys. Lett., 249(1996)105-111.

[56] G. R.J. Williams, J. Mol. Struct.: THEOCHEM, 151(1987)215-222.

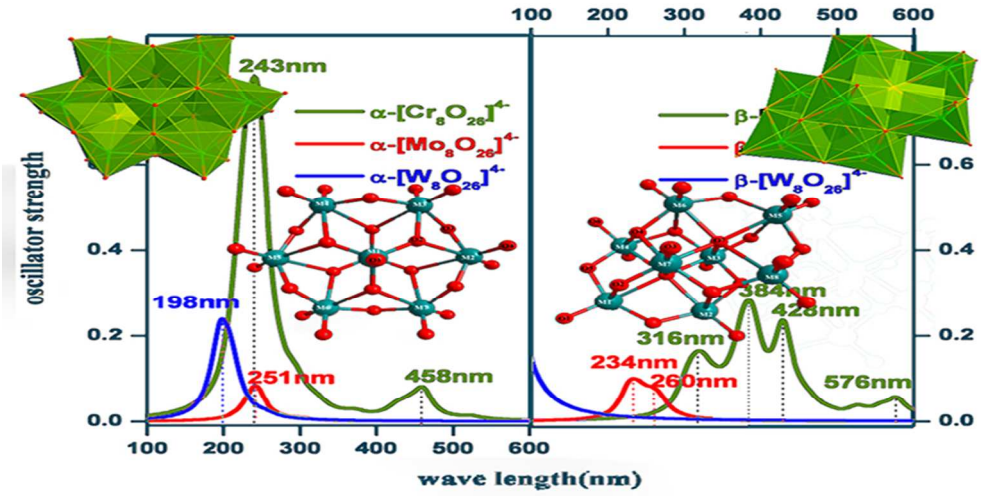

80x39mm (300 x 300 DPI)